

The Effect of *trans* Axial Isocyanide Ligands on Iron(II) Tetra-NHC Complexes and their Reactivity in Olefin Epoxidation

Eva-Maria H. J. Esslinger, Jonas F. Schlagintweit, Greta G. Zámbo, Alexander M. Imhof, Robert M. Reich, and Fritz E. Kühn^{*[a]}

Abstract: The performance of *trans* axially substituted mono- (2a) and bis(*tert*-butylisocyanide) (2b) complexes derived from the highly active bio-inspired iron(II) (pre-)catalyst 2 containing an equatorial macrocyclic tetra *N*-heterocyclic carbene in homogenous olefin epoxidation catalysis is reported. H₂O₂ is used as oxidant in combination with the Lewis acid Sc(OTf)₃ as additive resulting in a considerable

improvement of catalytic activity. In contrast to other iron epoxidation catalysts, the introduction of π -accepting isocyanide ligands does not improve the catalytic performance of 2a and 2b posed by cyclic voltammetry. However, besides their lower activity, a high temperature tolerance of both compounds is found as a unique feature for iron NHC epoxidation catalysts.

Introduction

Oxidation catalysis, especially the oxidation of olefins to epoxides as wide-ranging intermediates plays a pivotal role in polymer industry as well as in the production of fine chemicals, food additives, and drug intermediates.^[1]

As electronic and catalytic properties are mainly influenced by the choice of the central metal and the surrounding ligand sphere, a variety of catalysts have been designed and tested over time. Among them, many homogeneous catalysts based on expensive noble metals such as palladium, rhodium, molybdenum, rhenium, and ruthenium are characterized by high efficiency in several applications.^[2] With regards to economic costs and the rising interest in sustainable catalysis,^[3] the use of earth-abundant and non-toxic transition metals came more into focus.^[4] Iron is the most common transition metal in the earth's crust (4.7 wt%) and in living organisms with iron cofactors that are capable to catalyse manifold oxidation reactions from demanding C–H activation to *cis*-dihydroxylation and epoxidation with high selectivity and activity at mild conditions.^[2b,4–5] Thus, using nature as a role model led to the mimicking of heme and non-heme iron complexes^[6] and their application in the oxidation of organic molecules.^[7] Cytochrome P450 (CYP), one of the most intensively studied oxygen-activating superfamily of heme-containing enzymes, enables

the controlled hydroxylation of aliphatic C–H bonds and the epoxidation of C=C double bonds with high regio- and stereoselectivity.^[6,8] These natural systems have an iron-porphyrin core^[9] as a key structural motive in common, based on a Fe(II/III) center and coordinating polydentate, mostly tetradentate *N*-donor ligands.^[6] Due to the mentioned structure-activity insights, the synthesis and application of *N*-heterocyclic carbene (NHC) ligands with easy-to-modify steric and electronic properties have become increasingly interesting for transition-metal centers in oxidation catalysis.^[10] A wide range of these artificial bio-inspired iron catalysts exhibit an octahedral structure of iron(II) complexes with two labile ligands (e.g. solvent molecules) in *cis* or *trans* position to each other, determined by the coordination mode of the NHC ligand, containing amine, pyridine, pyrrolidine, and pyrrole units.^[5a,11]

Since reaction performance under aerobic conditions (activation of dioxygen in nature often involving cofactors like NADPH/H⁺ as reducing agent)^[8b] is often difficult to control, hydrogen peroxide has become an established alternative as an oxidant in catalytic reactions. Besides its relatively high atom efficiency (47%), water is generated as the only by-product making it an environmentally friendly oxidant^[5a,12] in contrast to other sources such as Peroxysulfates,^[13] Hypochlorites,^[14] or Periodates.^[15] First of all, the reaction of the Fe-complex with hydrogen peroxide initiates the formation of an iron(III) hydroperoxo intermediate by a ligand exchange reaction after an essential one electron step (Fenton).^[11b,16] According to mechanistic studies, either a high valent iron(V)-oxo compound or an iron(IV)-oxo species with an oxyl radical can be formed in the following step depending on a homolytic or heterolytic cleavage pathway. The latter is less preferred as electron-deficient oxidants like H₂O₂ do not have stabilizing ability for the resulting radical, rendering it incapable to attack the oxygen source and the catalyst.^[11b,16] Furthermore, the interplay of the ligand arrangement (*cis/trans*) at the central atom and selectivity emphasize the competing character between dihydroxylation and epoxidation.^[17] Complexes with *cis*-oriented ligands tend more to dihydroxylation, whereas epoxidation takes rather

[a] E.-M. H. J. Esslinger, J. F. Schlagintweit, G. G. Zámbo, A. M. Imhof, Dr. R. M. Reich, Prof. Dr. F. E. Kühn
Molecular Catalysis, Catalysis Research Center and Department of Chemistry
Technische Universität München
Lichtenbergstrasse 4, D-85748 Garching bei München (Germany)
E-mail: fritz.kuehn@ch.tum.de

Supporting information for this article is available on the WWW under <https://doi.org/10.1002/ajoc.202100487>

© 2021 The Authors. Asian Journal of Organic Chemistry published by Wiley-VCH GmbH. This is an open access article under the terms of the Creative Commons Attribution Non-Commercial NoDerivs License, which permits use and distribution in any medium, provided the original work is properly cited, the use is non-commercial and no modifications or adaptations are made.

place when the labile sites are in *trans* position.^[11a] It has been observed, that the activity of the catalysts of the type described in this work can be noticeably improved by additives, such as Lewis (*e.g.* scandium(III)-triflate) or Brønsted (*e.g.* perchloric, acetic acid) acids.^[18] The presence of additives is supposed to facilitate the O–O bond heterolysis towards the formation of a highly electrophilic active species.^[18a,19] The suppressing effect of Sc³⁺ on the deactivation pathway leading to an oxo-bridged Fe^{III}–O–Fe^{III} species of a non-heme iron-NHC-complex epoxidation reaction is also another essential point with regard to a significant increase of the turnover number.^[20]

Well-studied prototypes of successful artificial catalytic models are primarily represented by bio-inspired iron-complexes **1** and **2** bearing tetradentate NHC ligands (Figure 1).^[10,21a]

Their applicability as catalyst precursors includes a variety of transformations such as the oxidation of unreactive alkanes, aromatic hydroxylation, and olefin epoxidation.^[10a,21a]

Complex **1**, bearing a bis(pyridyl-NHC) ligand NCCN was the first organometallic iron complex (with a Fe–C bond) used for epoxidation reactions enabling high activity and selectivity.^[22] Compared to **1**, complex **2** and its Fe(III) derivative, bearing a tetradentate macrocyclic NHC ligand cCCCC has been standing out with particularly high activity (turnover frequencies up to 183,000 h⁻¹) and in comparison to other iron catalysts high turnover numbers (TON up to 4,300). Here again, the activity-rising-effect of additives (largely doubling TOFs to values up to 410,000 h⁻¹) by applying Sc(OTf)₃, Ce(OTf)₄, or Fe(ClO₄)₃·H₂O on complex **2** is of high relevance in epoxidation catalysis.^[20] These reference points showcase again the competitive potential of iron complexes over more expensive metal catalysts.^[4]

Specific electronic and hence associated catalytic characteristics (activity, selectivity, stability) of the complexes can be obtained by variation of the polydentate scaffold or the introduction of ligands with individual electron pulling or pushing properties.^[21a] Concerning this matter, the influence of axial ligands on catalytic properties through axial ligand exchange at accessible coordination sites has been thoroughly investigated by cyclic voltammetry (CV) experiments concerning the Fe–NCCN complex **1**.^[21a] The result is a better catalyst

performance, recognizable by an increase in selectivity and turnover number in the precious C–H-oxidation of alkanes^[23] by introduction of a *tert*-butyl isocyanide ligand (**1a**) with π -acceptor and σ -donor features at one coordinating site of the complex.^[21] On account of the easily modifying functionality, isocyanides were synthetically favored instead of their isolobal CO counterpart.^[10a,21a] Increasing the substitution grade from 1 to 3 π -accepting isocyanide ligands at complex **1** (**1e–h**) (two-isocyanide substituted complexes could not be isolated) has resulted in an increase of the half-cell potential ($E_{1/2}$ = 0.57 V–1.092 V).^[21a] With respect to this observed tendency, all iron NHC complexes in olefin epoxidation display a typical correlation pattern between the redox potential and the resulting catalytic activity. Thus, a lower half-cell potential of the reversible Fe(II)/Fe(III) redox couple indicates a higher activity and vice versa.^[4,22,24]

This concept of isocyanide ligand substitution was transferred to the notably more active Fe–cCCCC complex **2** to create novel complexes with mixed catalytic properties released by axial π -acceptor ligands.^[4,21b] Accordingly, the mono- (**2a**) and bis(*tert*-butylisocyanide) derivatives (**2b**) were already synthesized and characterized by NMR-spectroscopy, elemental analysis, ESI-MS, and single crystal X-ray diffraction (SC-XRD) before.^[21b] Preceding cyclic voltammetry studies of both new compounds reveal the same redox potential trend, rising from mono- to bis(*tert*-butylisocyanide) ligand substitution. In comparison to **2** ($E_{1/2}$ = 0.15 V) and **2a** ($E_{1/2}$ = 0.35 V), **2b** displays the highest half-cell potential ($E_{1/2}$ = 0.44 V) corresponding to the reversible Fe(II)/Fe(III) redox process.^[21b] Another derivative **3** with a tetradentate macrocyclic NHC ligand cCCCC (Figure 2) showing similar electrochemical properties ($E_{1/2}$ = 0.44 V) is also examined and serves as an interpretation basis for the obtained catalytic results of **2a** and **2b**. Compared to **2a** and **2b**, complex **3** is bearing a backbone-modified imidazole structure without any modification at the axial positions.^[25]

The characteristic macrocyclic benzimidazolylidene ligand is inducing lower electron-donating properties because of the enlarged aromatic ring system and provokes analogously a decreased electron density at the iron center, but through

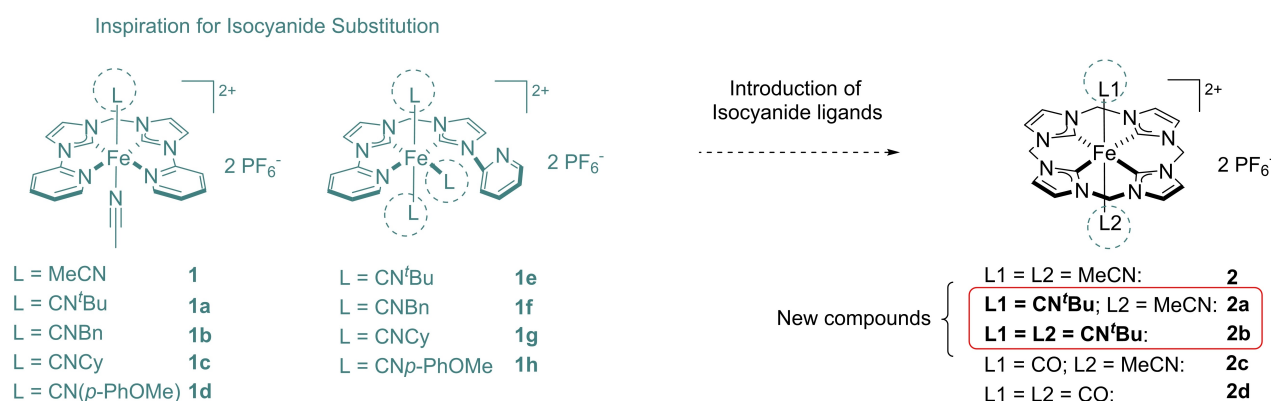


Figure 1. Structures of iron(II) complexes **1a–1d** containing tetradentate bis(pyridyl-NHC) ligand NCCN and one isocyanide ligand and **1e–1h** containing tridentate NCCN and three isocyanide ligands (left).^[21] Structures of complex **1** as an example for the application of one or two isocyanide ligands at complex **2** leading to mono- and bis(*tert*-butylisocyanide) substituted derivatives **2a** and **2b**. Their isolobal carbonyl analogs **2c** and **2d** containing tetradentate macrocyclic NHC ligand cCCCC are also depicted (right).^[10a,21b]

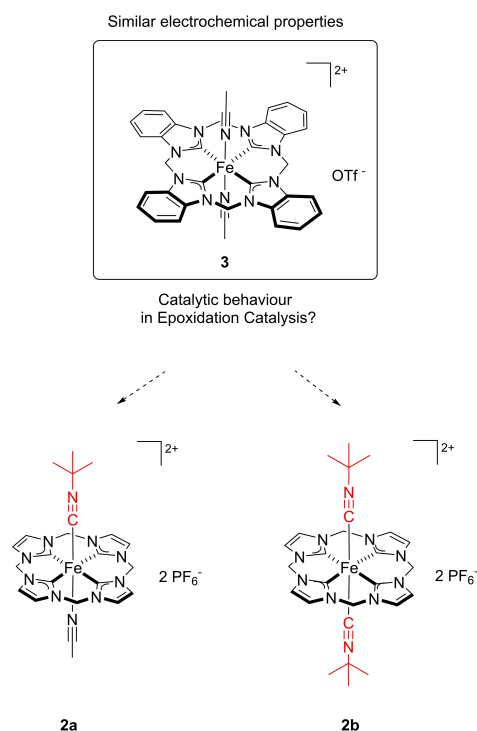


Figure 2. Comparison of the mono- and bis(*tert*-butylisocyanide) substituted derivatives **2a** and **2b** with an already existing and in epoxidation catalysis tested system **3**.^[25]

equatorial modification.^[25] These electronic features are reflected in an overall lower activity, high turnover numbers and especially in a light increase in stability towards higher temperatures in epoxidation catalysis.^[25] In this work, compounds **2a** and **2b** are applied in olefin epoxidation catalysis as a means of confirming the described redox behavior and its degree of influence on higher TONs as for complex **3**. Looking at the diversity of chemical features including compounds **1**, **2**, their derivatives, and compound **3**, the novel compounds **2a** and **2b** are expected to be unique in their catalytic performance. Furthermore, UV/Vis spectroscopy and thermogravimetric analysis of compounds **2a** and **2b** should reinforce the catalytic results and are also reported in this work.

Results and Discussion

Catalytic Olefin Epoxidation

Complexes **2a** and **2b** are studied in terms of their applicability as catalysts in olefin epoxidation reactions. Their performance is compared to the most active literature known non-heme iron complexes **1** and **2** as well as to complex **3** which possess similar electrochemical features (room temperature). Under standard conditions, H₂O₂ is applied as oxidant, acetonitrile as solvent, and *cis*-cyclooctene as a model substrate.

GC-FID analytic method is applied for the model substrate, particularly for the quantification of the formed epoxide and the respective *cis*-diol as a common byproduct. The catalytic

performance of both new compounds related to other substrates is conducted *via* ¹H-NMR spectroscopy.

When evaluating the curve progression, specifically the curve slope of (pre-)catalysts **2a** and **2b** in view of conversion [%] and yield [%] at 20 °C, it is obvious, that the mono-(*tert*-butylisocyanide) substituted derivative **2a** reveals a higher catalyst activity compared to the bis-(*tert*-butylisocyanide) substituted derivative **2b** (Figure 3). Hence, the activity estimation with the aid of half-cell potentials of each compound still remain a solid comparative basis. This is underlined by considering the reaction time (~12 h) of **2a**, which is about twice as high as for **2b** (~6 h). Moreover, this finding in terms of the catalytic reaction rate is supported by specific turnover numbers of **2a** (TON=84) and **2b** (TON=72) at a catalyst concentration of 1.0 mol%. However, the combination of a high catalyst concentration (1.0 mol%) and the necessary usage of scandium(III)-triflate as an additive demonstrates an overall low activity, but appropriate higher stability for both catalysts in the epoxidation reaction. These findings can be explained through the different substitution grades with *trans* axial *tert*-butylisocyanide ligands at the iron center. First, accessible coordination sites must be present for the attack of the oxidant in order to form the active species.^[11b] Accordingly to the examined reversibility of the redox process in cyclic voltammetry for compound **2b**, no isocyanide ligand dissociation after the oxidation step is expected, so that ligand exchange reactions at the beginning are hampered.^[21b]

Even the reduced π -backbonding at the iron center because of two competing axial isocyanide ligands with π -acceptor character leads only to weak dissociation of the ligands in acetonitrile, determined by ¹H-NMR spectroscopy.^[21b] Contrarily, the more active (pre-)catalyst **2a** exhibits one accessible coordination site with a weakly coordinating acetonitrile ligand which can be easily exchanged. Nevertheless, the π -backbonding from the iron center is reinforced by the stronger electron donating cCCCC-scaffold compared to NCCN and shortens the Fe–C_{isocyanide} bond so that the dissociation of the isocyanide ligand is impeded. This could explain the limited catalyst activity of **2a** despite the freely accessible coordination site.^[21a] As can be observed in both cases, the reaction needs a strong additive as first initiator, otherwise barely low or rather no conversion can be noticed if only H₂O₂ interacts with the catalyst (Figure 3). This indicates that Sc(OTf)₃ does not only accelerate the O–O-cleavage of the formed iron(III) hydroperoxo intermediate,^[18a] but also accelerates the formation of a free coordination position at the iron center, which is also confirmed by UV/Vis spectroscopy (see SI for further information). A closer look at conversion and yield of both catalysts reveals that no high selectivities are achieved. *Via* GC-FID analysis, many unidentifiable side-products besides small amount of *cis*-diol, explaining the gap between the conversion and yield graphs can be detected with help of the respective chromatograms.

Reducing the temperature provides further insights into existing induction periods of both compounds. In terms of the extremely low catalyst activities, a temperature of 0 °C instead of –10 °C or –20 °C as for other known high performance catalysts is chosen (Figure 4).^[4,24]

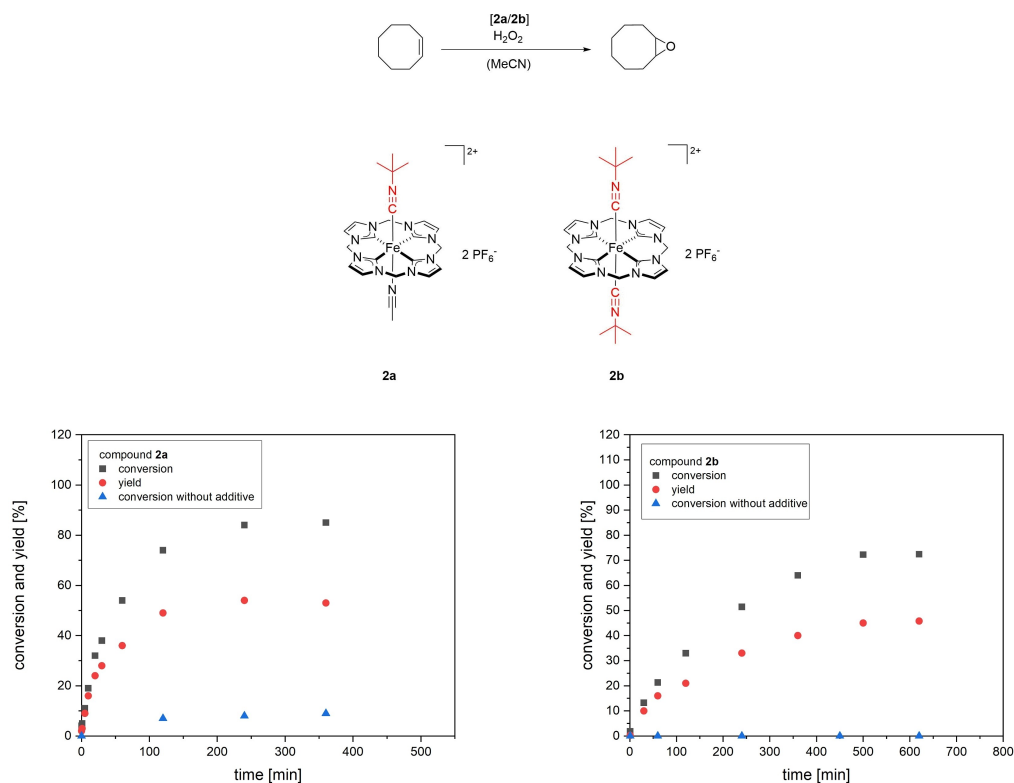


Figure 3. Conversions and yields (*cis*-cyclooctene oxide) applying catalysts (1.0 mol%) **2a** at 20 °C (left) and **2b** at 20 °C (right) in olefin epoxidation of *cis*-cyclooctene in absence and presence of Sc(OTf)₃.

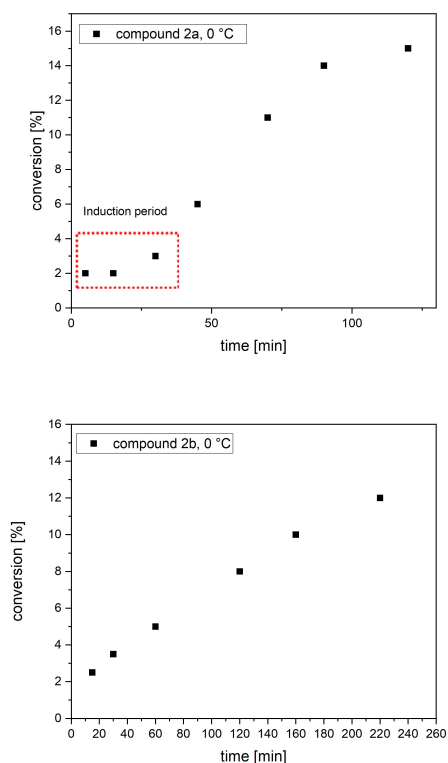


Figure 4. Conversions of cyclooctene applying catalysts (1.0 mol%) **2a** (above) and **2b** (below) at 0 °C in olefin epoxidation of *cis*-cyclooctene in presence of Sc(OTf)₃ in order to determine the existence of an induction period. The approximate length of the induction period is marked in red.

While the curve shape for complex **2b** shows an almost linear path, a slight induction period for complex **2a** can be observed. The length of the induction period is about 30 min (Figure 4) in spite of the presence of Sc(OTf)₃ and highlights the overall low activity associated with a slow oxidation step from Fe(II) to Fe(III) towards more active catalyst species.^[4,25] The oxidation to the active species in case of complex **2b** seems to be extremely slow so that the key reaction, the epoxidation of *cis*-cyclooctene may outperform the rate-determining step resulting in a curve linearity.

Due to the overall low catalytic performance of both compounds, the reaction temperature is increased from 20 °C to 40 °C and 60 °C with the focus on the development of the catalyst activity (TOF) and catalyst stability (TON) (Figure 5). It is clear that the TOF numbers of each catalyst are rising at elevated temperatures and that the reaction time is highly reduced to a time range of 15 min to max. 120 min for both compounds. Consequently, the reaction is already completed after 15 min for **2a** and after 30 min for **2b** in the fastest case (60 °C) at a catalyst concentration of 1.0 mol% in combination with Sc(OTf)₃.

In order to determine max. TOFs, a catalyst concentration of 0.25 mol% is used for **2a** and **2b** (Table 1). The results achieved at different temperatures show a rapid increase of the TOF from 1,400 h⁻¹ to 25,900 h⁻¹ for complex **2a** and demonstrate its already examined higher catalytic activity. On the other hand, **2b** also shows a rather low increase of activity displayed in its TOF indicating a considerable higher stability towards increas-

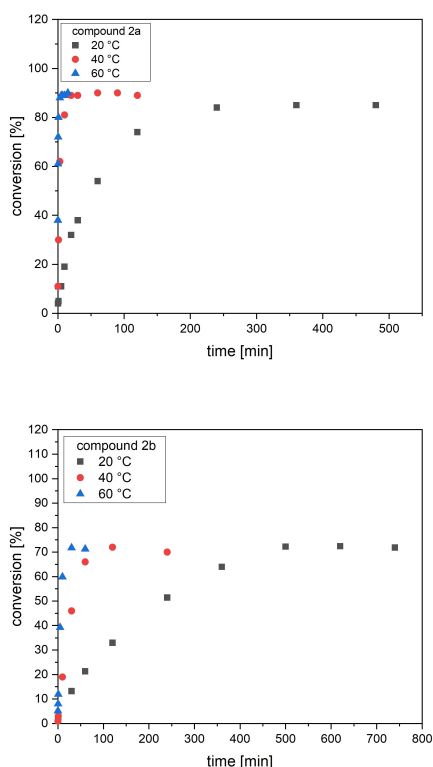


Figure 5. Conversions of cyclooctene applying catalysts (1.0 mol%) **2a** (above) and **2b** (below) at 20 °C, 40 °C and 60 °C in olefin epoxidation of *cis*-cyclooctene in presence of Sc(OTf)₃.

Table 1. Catalytic performance of catalysts **2a** and **2b** in the epoxidation of *cis*-cyclooctene in comparison to catalysts **1**, **2** and **3**.

catalyst	T [°C]	conv. [%] ^[a]	yield [%] ^[a]	sel. [%] ^[a]	TOF [h ⁻¹] ^[b]
2a	20	85	54	83	1 400*
2a	40	90	58	71	6 200
2a	60	90	52	59	25 900
2b	20	72	46	75	240
2b	40	72	45	72	2 900
2b	60	72	41	59	4 300
1 ^[c]	20	66	66	> 99	792
2 ^[c]	20	24/59 ^[d]	100	> 99	50.000/ 415.000 ^[d]
3 ^[c]	20	100	96	96	11.000 ^[e]

Reaction conditions: *cis*-cyclooctene (269 μmol, 1.0 eq.), Sc(OTf)₃ (26.9 μmol, 0.1 eq.), H₂O₂ (403 μmol, 1.5 eq.), catalyst (2.69 μmol, 1.0 mol%); [a] all yields (*cis*-cyclooctene oxide) and conversion were determined by GC-FID after the completion of the reaction; [b] Max. TOFs were determined at a catalyst concentration of 0.25 mol% at 20 °C, 40 °C and 60 °C for catalyst **2a** and **2b**. [c] **1** & **3**: catalyst concentration of 1.0 mol%. **2**: 0.05 mol% without additive. [d] with additive Sc(OTf)₃. [e] TOF number of Fe(III) species. * catalyst concentration of 1.0 mol% for **2a** at 20 °C. Blank experiments (reaction mixture **1**) without iron catalysts and with **2**) a simple iron salt) are included.

ing temperatures along with a low level of activity based on its substitution with two weakly dissociating *tert*-butylisocyanide ligands in axial position.

Compared to the first investigated classical cCCCC and NCCN systems,^[4,22] the determined TOFs of **2a** and **2b** do not reach the same level of activity of these previously in literature reported catalysts, even by using an additive (Table 1). How-

ever, catalyst **2a** (1.0 mol%) with a max. TOF of 1,400 h⁻¹ at 20 °C lies in between these two systems, but remains all in all in the lower area of potential achievable TOF numbers.

A particularly conspicuous new aspect among all existing iron epoxidation catalysts is the widely constant TON observed at higher temperatures. The TON in case of **2a** and **2b** remains largely identical within the margin of error from 20 °C to 60 °C (Table 1, Figure 6). These outcomes demonstrate once again the exceptionally high temperature stability of both complexes, in particular of complex **2b**. The temperature consistency and the associated high stability contrast with the low catalyst activity, which may constitute the limiting factor with respect to the average TON values, especially for complex **2b**. Reducing the catalyst concentration (0.1 mol%) leads to max. TONs up to 330 for **2a** and 150 for **2b**. Thus, rising temperatures may have a stronger impact on lower catalyst concentrations, major fluctuations can be seen at a catalyst concentration of 0.1 mol% compared to 1.0 mol% (Figure 6).

Simultaneously, a generally decline of yield and selectivity for compound **2a** and **2b** (Table 1) can be explained by the fact that another reaction type, competing with the epoxidation takes place as no further *cis*-diol formation can be noticed in comparison to catalytic reactions at 20 °C, attributable to the growing activity and remaining stability at higher temperatures. Conceivable would be, that these features may orient the catalyst selectivity to more challenging substrates as for example in the C–H oxidation. Analogous to derivative **3**

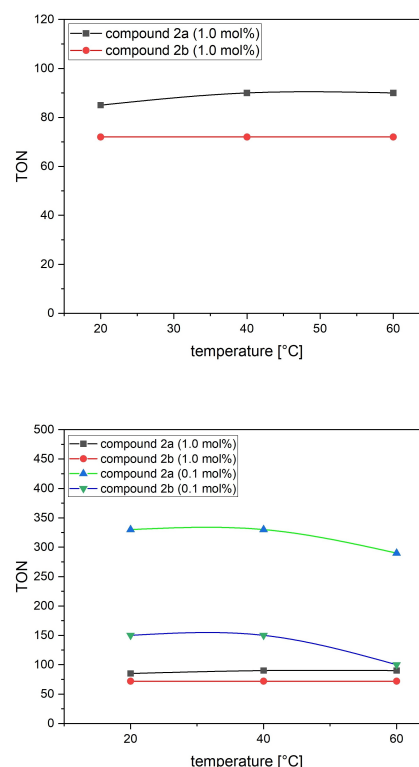


Figure 6. Comparison of TONs of catalysts (1.0 mol%) **2a** and **2b** at various elevated temperatures in presence of Sc(OTf)₃ (above). All TONs were determined at catalysts concentrations of 1.0 mol% and 0.1 mol% for maximum achievable values (below).

(Figure 1), bearing a characteristic tetradentate macrocyclic benzimidazolylidene ligand, catalysts **2a** and **2b** show high stability combined with a high temperature tolerance (up to 60 °C), but an overall lower activity in contrast to the most active non-heme iron epoxidation catalyst to date (**2**) due to the electronic-finetuning at the iron center or the modified scaffold in case of **3**.^[25] Interestingly, the initial oxidation step of catalyst **3** from Fe(II) to Fe(III) is slowed down by the withdrawing properties of the modified scaffold, coinciding with the significantly higher half-cell potential ($E_{1/2}=0.44$ V).^[25] This fact can be transferred to the more active mono-*tert*-butylisocyanide substituted compound **2a** having a nearly related half-cell potential ($E_{1/2}=0.35$ V), resulting in a long-lasting induction period even in the presence of $\text{Sc}(\text{OTf})_3$.^[25]

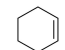
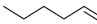
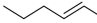



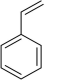
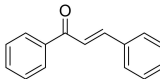
Moreover, the better catalyst performance of **3** compared to **2a** and **2b**^[25] is a good indication of the exact location for the selective modification at the classical iron NHC complex with two axial acetonitrile ligands. Direct modifications on the base frame or the iron center obviously evoke widely divergent features with regard to the catalytic activity.

For a broad understanding concerning the catalytic potential of **2a** and **2b**, supplementary epoxidation reactions with various cyclic, acyclic, terminal and functionalized olefin substrates are conducted via ¹H-NMR spectroscopy (SI, Figures 1–17). All experiments are realized using 1.0 mol% of the respective Fe(II)-catalyst and 0.1 eq. $\text{Sc}(\text{OTf})_3$ at 20 °C with a reaction time of approximately 24 h. Due to the overall low activity of both catalysts and the crucial necessity of $\text{Sc}(\text{OTf})_3$ as additive, a comparatively long reaction time is chosen for maximal achievable conversions and yields (Table 2). For better

control of the reaction progression over a longer time period, the setting of higher temperatures is avoided. To obtain suitable NMR spectra, the overall concentration is doubled. By means of the ¹H-NMR experiments, it becomes visible, that catalysts **2a** and **2b** are capable to reach conversions up to 73% for more challenging double bond systems except for the substrate allyl chloride (entry 6). As the formed active species in epoxidation catalysis possesses an electrophilic oxygen,^[11c] the electron density of the double bond plays a decisive role in the reactivity of the relevant substrate. The chloride substituent at entry 6 exerts a negative inductive effect and leads to a lower electron density, which finally impedes the desired electrophilic attack of the active species.

If the chloride substituent is replaced by an electron-donating hydroxyl group (entry 5), conversions up to 42% are feasible due to the increased electrophilic character of the double bond. The highest conversion is obtained for hex-2-ene (entry 3) as another acyclic system with 73% followed by allylic alcohol (entry 5) and styrene (entry 7) as an aromatic system with 38%. Hex-2-ene (entry 3) has an increased reactivity based on the fact, that the internal double bond is affected by neighboring alkyl groups as opposed to 1-hexene (entry 2) and 1-octene (entry 4) with less reactive terminal double bonds. Styrene (entry 7) contains an aromatic system, which can apparently better stabilize the formed epoxide product, whereas *trans*-chalcone (entry 8) bears additionally an electron-withdrawing carbonyl group close to the double bond, provoking a reduced electron density. As observed in the catalytic epoxidation of *cis*-cyclooctene, the more active catalyst **2a** reaches higher conversion and selectivity in comparison to **2b**. With respect to the resulting conversions, the epoxide yields of all investigated substrates, leading to maximal selectivities of 23% are negligible, which again supports the assumption, that another reaction type potentially interferes. Concerning this matter, a divergent behavior pattern of **2a** and **2b** referring to other cyclic substrates like cyclohexene (entry 1) is basically recognizable when compared to other non-heme catalysts.^[4,24–25] Usually, cyclic olefins are considered as favored substrates in epoxidation reactions as the electron donating effect of the neighboring CH_2 -groups. Contrary to the assumptions, the oxidation products of the catalyzed cyclohexene are not just limited to the formation of *cis*-diol, but also arise from oxidation of existing C–H bonds and can be assigned by NMR spectroscopy to several ketone (2-cyclohexen-1-one) and alcohol (2-cyclohexen-1-ol) species nearby located to the double bond. Apart from the new findings, *cis*-diol appears in nearly all cases as one of the main side products and emphasize the unfavored epoxide formation, probably inhibited by the present $\text{Sc}(\text{OTf})_3$, which is able to open epoxides to *cis*-diols in presence of water unlike coordinating Brønsted acids.^[18b] However, due to the high amounts of existing co-products, the signal assignment remains mainly an assumption. The appearance of new functional groups as ketones, alcohols and aldehydes like acrolein for entry 5 and benzaldehyde in the case of entries 7 and 8 clearly underlines the expected significant low selectivity towards more challenging substrates in olefin epoxidation. The NMR experiments are also conducted for the standard substrate

Table 2. Catalytic epoxidation of various olefins by catalyst **2a** and **2b**.

entry	substrate	2a conv. [%]	2a sel. [%] ^[a]	2b conv. [%]	2b sel. [%] ^[a]
1		19	5 ^[b]	19	5 ^[b]
2		30	23	23	17
3		73	8	58	5
4		14	14	14	14
5		42	– ^[c]	42	– ^[c]
6		–	–	–	–
7		38	3 ^[c]	35	3 ^[c]
8		12	– ^[c]	12	– ^[c]

Reaction conditions: substrate (135 μmol, 1.0 eq.), $\text{Sc}(\text{OTf})_3$ (13.5 μmol, 0.1 eq.), H_2O_2 (aq. 50%, 202 μmol, 1.5 eq.), **2a** & **2b** (1.0 mol%), solvent MeCN-d_3 , $t_r=24$ h, $T_r=20$ °C; conversions and selectivities are identified by ¹H-NMR spectroscopy applying benzol (entry 1–6) and toluene (entry 7, 8) as external standard; [a] *cis*-diol formation and identified high amounts of byproducts with new functional groups as ketones, alcohols and aldehydes (see SI for further information); [b] possible side products of the catalyzed cyclohexene: 2-cyclohexen-1-one and 2-cyclohexen-1-ol; [c] aldehyde formation to acrolein (entry 5) and benzaldehyde (entries 7 & 8).

cis-cyclooctene under the same conditions and showed similarly to cyclohexene, the formation of C–H oxidation products as well. This outcome confirms the former detection of several side products *via* the quite more sensitive gas chromatography (see SI for further information) and may switch the future focus on investigations of C–H-oxidations with the catalysts **2a** and **2b**.

Thermogravimetric Analysis (TGA)

In regards to the unusual high tolerance of catalyst **2a** and **2b** to increased temperatures in epoxidation catalysis, thermogravimetric measurements were conducted for catalyst **2**, **2a** and **2b** in solid state (Figure 7).

The thermal stability of all three compounds is determined through monitoring the weight change by heating the sample at a constant rate of 10 K/min in a temperature range from 25 °C to 300 °C. The heating chamber where the respective catalyst is placed, is purged with nitrogen with a volume flow of 100 ml/min. Initial irregularities arise from small fractions of volatile components. Thus, the samples are examined in solid state, catalytic reaction conditions in solution can not be imitated realistically on account of the respective components (e.g. oxygen, H₂O₂, additives) which influence or rather reduce the actual thermo-stability of the catalysts during the reaction, so that the real decomposition process under catalytic conditions possibly occurs at lower temperatures. Nevertheless, a general trend of the catalyst decomposition in temperature dependency is essential for further interpretation. Catalyst **2** decomposes already at 155 °C, while the decomposition onset of compounds **2a** and **2b** is detected at 185 °C and 225 °C, respectively. This observation supports the catalytic results relating to unvarying turnover numbers coming from a high temperature tolerance, corresponding to following catalytic activity order: **2** > **2a** > **2b**.

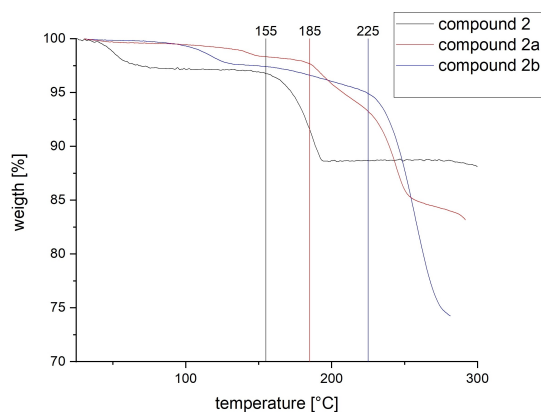


Figure 7. Thermogravimetric analysis of catalyst **2**, **2a** and **2b** and determination of the dissociation temperature in solid

Conclusion

The previous estimation of an overall lower catalyst activity by CV data could be largely confirmed by means of the catalytic epoxidation reaction of *cis*-cyclooctene with *trans* axially substituted mono (**2a**) and bis(*tert*-butylisocyanide) (**2b**) (pre-) catalysts. According to the comparison of half-cell potentials, the catalytic activity of **2a** and **2b** should be between that of the iron(II) complex **2** bearing a macrocyclic tetra-NHC ligand cCCCC and *trans* labile acetonitrile ligands and the iron(II) complex **1** with a tetradentate bis(pyridyl-NHC) ligand NCCN, also bearing *trans* labile acetonitrile ligands. Contrary to expectations, both complexes **2a** and **2b** show comparatively low activities correlating to their electrochemical properties, which are highly influenced by the isocyanide ligands with π -accepting character. This finding is supported by the necessary use of Sc(OTf)₃ as an additive in order to activate the (pre-)catalysts for the epoxidation of olefins. Due to the fact that **2a** possesses one accessible coordination site with a weakly coordinating and hence easily replaceable acetonitrile ligand, an increased activity compared to **2b** with two comparatively weak dissociating isocyanide ligands is found. The stronger electron donating cCCCC scaffold compared to NCCN makes the dissociation of one isocyanide ligand rather difficult, resulting from the reinforced π -backbonding from the iron center and could explain the limited catalyst activity of **2a** towards other non-heme iron(II) catalysts despite the freely accessible coordination site. Rising temperatures effect increased activities, manifested by a significant development of the TOF values from 1,400 h⁻¹ to 25,900 h⁻¹ for **2a** and 240 h⁻¹ to 4,300 h⁻¹ for **2b**. Thereby, a particular new aspect is the consistent TON and consequently high stability of the catalysts at different temperature levels such as (pre-)catalyst **3** with analog electrochemical features, but equatorially placed modifications. High decomposition temperatures, especially for **2b** specified by TGA measurements correlate well with an observed great temperature tolerance during epoxidation reaction. As a whole, the compound is also exceptionally stable in solid state in addition to a high temperature stability under oxidative conditions compared to various other iron NHC catalysts.

An overall higher catalyst performance of **3** evidently makes a difference if new functional groups with unique electron properties are introduced axially or equatorially to the iron center where the initial oxidation step takes place.

Related to selectivities in epoxidation reactions, a clear gap between the conversion and the yield can be observed for both catalysts **2a** and **2b**, pointing out a relatively high amount of unidentifiable side products apart from the minimal formation of *cis*-diol detected by gas chromatography. Finally, the presented catalytic experiments are considered essential for future improvements of catalyst activities (TON) and stabilities (temperature tolerance) based on the modification location and redox potentials. Additional substrate screening with more challenging olefins leads – not unexpectedly – to low yields and selectivities regarding epoxide formation. The unusual formation of C–H oxidation products, particularly in the case of cyclohexene is additionally supporting the assumption of

another competing reaction type. Inspired by NCCN ligand derivatives **1a–1d**, showing improved turnover numbers in the C–H oxidation reaction after replacing one labile acetonitrile ligand through one isocyanide ligand, the same substitution pattern at (pre-)catalyst **2** might have enhanced the potential for activating unreactive alkanes for the challenging C–H oxidation and may be worth further examination.

Experimental Section

General Procedures and Analytical Methods

All reagents and solvents for the catalytic procedures were purchased from commercial suppliers and used without further purification. NMR spectra were recorded on a Bruker AV 400 (¹H-NMR, 400.13 MHz) and chemical shifts are reported relative to the residual signal of the deuterated solvent. UV-Vis spectra were recorded on an Agilent Technologies Cary 60 UV-Vis spectrophotometer at 20 °C. Solutions of **2a** and **2b** with an initial concentration of 10⁻⁴ M in acetonitrile were treated with 10.0 eq. Sc(OTf)₃ and 1.50 eq. H₂O₂.

Catalytic procedures

All reactions were conducted in a cryostat (Julabo FP-50) with a total reaction volume of 4.0 mL. Acetonitrile (HPLC-grade) as solvent was applied for all experiments. The catalyst (1.0 mol%, 2.69 μmol) was added from a preformed stock solution (5.5 mg/mL in acetonitrile) corresponding to the appropriate stoichiometry to a solution of *cis*-cyclooctene (100 mol%, 269 μmol) and, if applied, the respective Brønsted acid (0.1 mol%, 26.9 μmol) in acetonitrile. The reaction was started upon addition of H₂O₂ (150 mol%, 403.5 μmol). The reaction was terminated by adding electrolytically precipitated activated MnO₂ in order to decompose the excess of H₂O₂ in the reaction solution. After filtration over activated neutral alumina (separation of the catalyst), two GC samples were prepared for each experiment using 200 μL filtrate, 500 μL external standard (*p*-xylene, 4.0 mg/mL in *i*-PrOH) and 800 μL *n*-hexane for each chosen time point. Control experiments without catalyst were performed as a reference for all reactions. An additional blank experiment with a simple iron salt, iron(II) chloride in the presence of H₂O₂ was conducted in order to stress the relevance of iron complexes associated with NHCs due to minimal product and unselective side-product formation.

The screening of other substrates beside *cis*-cyclooctene was performed using ¹H-NMR spectroscopy. All reactions were carried out at 20 °C in a total volume of 1.0 mL with a catalyst concentration of 1.0 mol% in doubled absolute concentrations. A catalyst stock solution (5.5 mg/mL in CD₃CN) was added to a prepared solution of the respective substrate (100 mol%, 134.5 μmol) in deuterated acetonitrile and the reaction was started upon addition of H₂O₂ (150 mol%, 201.8 μmol). Then, the reaction was aborted after 24 h by adding electrolytically precipitated activated MnO₂. The suspension was filtered and benzol or toluene was added as an external standard. For each experiment, ¹H-NMR spectra were recorded and the products were quantified by integral ratios of the respective olefin, epoxide and *cis*-diol protons.

Thermogravimetric analysis

TGA measurements were recorded with a TGA/DSC 3+ from Mettler-Toledo. Approximately up to 5.0 mg of the respective

catalyst (**2a**, **2b**) were placed in a sapphire skillet attached to a microbalance. The heating chamber was purged with nitrogen with a volume flow of 100 mL/min. The thermal stability, especially the decomposition temperature of all three compounds was determined through monitoring the weight change by heating the sample at a constant rate of 10 K/min in a temperature range from 25 °C to 300 °C.

Acknowledgements

The authors thank the TUM graduate school of chemistry for financial support. Open Access funding enabled and organized by Projekt DEAL.

Conflict of Interest

The authors declare no conflict of interest.

Keywords: non-heme iron complexes · *N*-heterocyclic carbenes · isocyanide ligands · olefin epoxidation · homogeneous catalysis

- [1] a) A. Blanckenberg, R. Malgas-Enus, *Catal. Rev.* **2019**, *61*, 27–83; b) F. Cavani, J. H. Teles, *ChemSusChem* **2009**, *2*, 508–534; c) S. A. Hauser, M. Cokoja, F. E. Kühn, *Catal. Sci. Technol.* **2013**, *3*, 552–561.
- [2] a) S. Enthaler, K. Junge, M. Beller, *Angew. Chem. Int. Ed.* **2008**, *47*, 3317–3321; *Angew. Chem.* **2008**, *120*, 3363–3367; b) J. W. Kück, R. M. Reich, F. E. Kühn, *Chem. Rec.* **2016**, *16*, 349–364.
- [3] P. P. Chandrachud, D. M. Jenkins, *Tetrahedron Lett.* **2015**, *56*, 2369–2376.
- [4] J. W. Kück, M. R. Anneser, B. Hofmann, A. Pöthig, M. Cokoja, F. E. Kühn, *ChemSusChem* **2015**, *8*, 4056–4063.
- [5] a) K. Chen, M. Costas, J. Kim, A. K. Tipton, L. Que, *J. Am. Chem. Soc.* **2002**, *124*, 3026–3035; b) M. S. Chen, M. C. White, *Science* **2010**, *327*, 566–571.
- [6] L. Que, W. B. Tolman, *Nature* **2008**, *455*, 333–340.
- [7] A. Lindhorst, S. Haslinger, F. E. Kühn, *Chem. Commun.* **2015**, *51*, 17193–17212.
- [8] a) J. Rittle, M. T. Green, *Science* **2010**, *330*, 933–937; b) O. Shoji, Y. Watanabe, *Isr. J. Chem.* **2015**, *55*, 32–39.
- [9] a) I. D. Cunningham, T. N. Danks, J. N. Hay, I. Hamerton, S. Gunathilagan, C. Janczak, *J. Mol. Catal. A* **2002**, *185*, 25–31; b) S. Enthaler, G. Erre, M. K. Tse, K. Junge, M. Beller, *Tetrahedron Lett.* **2006**, *47*, 8095–8099; c) W. Nam, S.-Y. Oh, Y. J. Sun, J. Kim, W.-K. Kim, S. K. Woo, W. Shin, *J. Org. Chem.* **2003**, *68*, 7903–7906; d) W. J. Song, M. S. Seo, S. DeBeer George, T. Ohta, R. Song, M.-J. Kang, T. Tosha, T. Kitagawa, E. I. Solomon, W. Nam, *J. Am. Chem. Soc.* **2007**, *129*, 1268–1277; e) K. Srinivas, A. Kumar, S. S. Chauhan, *Chem. Commun.* **2002**, *20*, 2456–2457.
- [10] a) M. R. Anneser, S. Haslinger, A. Pöthig, M. Cokoja, J.-M. Basset, F. E. Kühn, *Inorg. Chem.* **2015**, *54*, 3797–3804; b) A. Raba, M. Cokoja, S. Ewald, K. Riener, E. Herdtweck, A. Pöthig, W. A. Herrmann, F. E. Kühn, *Organometallics* **2012**, *31*, 2793–2800.
- [11] a) Y. Feng, J. England, L. Que Jr, *ACS Catal.* **2011**, *1*, 1035–1042; b) S. M. Hölzl, P. J. Altmann, J. W. Kück, F. E. Kühn, *Coord. Chem. Rev.* **2017**, *352*, 517–536; c) W. Nam, *Acc. Chem. Res.* **2007**, *40*, 522–531.
- [12] a) R. Noyori, M. Aoki, K. Sato, *Chem. Commun.* **2003**, *16*, 1977–1986; b) N. A. Stephenson, A. T. Bell, *J. Am. Chem. Soc.* **2005**, *127*, 8635–8643.
- [13] a) B. De Poorter, M. Ricci, B. Meunier, *Tetrahedron Lett.* **1985**, *26*, 4459–4462; b) S. E. Denmark, D. C. Forbes, D. S. Hays, J. S. DePue, R. G. Wilde, *J. Org. Chem.* **1995**, *60*, 1391–1407.
- [14] a) D. Y. Kim, Y. J. Choi, H. Y. Park, C. U. Joung, K. O. Koh, J. Y. Mang, K.-Y. Jung, *Synth. Commun.* **2003**, *33*, 435–443; b) B. Meunier, E. Guilmet, M. E. De Carvalho, R. Poilblanc, *J. Am. Chem. Soc.* **1984**, *106*, 6668–6676.
- [15] B. Bahramian, V. Mirkhani, M. Moghadam, S. Tangestaninejad, *Catal. Commun.* **2006**, *7*, 289–296.
- [16] F. G. Gelalcha, *Adv. Synth. Catal.* **2014**, *356*, 261–299.

- [17] R. Mas-Ballesté, M. Costas, T. Van Den Berg, L. Que Jr, *Chem. Eur. J.* **2006**, *12*, 7489–7500.
- [18] a) S. Kal, A. Draksharapu, L. Que Jr, *J. Am. Chem. Soc.* **2018**, *140*, 5798–5804; b) R. Mas-Ballesté, L. Que, *J. Am. Chem. Soc.* **2007**, *129*, 15964–15972.
- [19] a) S. Kal, L. Que Jr, *Angew. Chem.* **2019**, *131*, 8572–8576; *Angew. Chem. Int. Ed.* **2019**, *58*, 8484–8488; b) M. Swart, *Chem. Commun.* **2013**, *49*, 6650–6652.
- [20] F. Dyckhoff, J. F. Schlagintweit, R. M. Reich, F. E. Kühn, *Catal. Sci. Technol.* **2020**, *10*, 3532–3536.
- [21] a) S. Haslinger, A. Lindhorst, J. Kück, M. Cokoja, A. Pöthig, F. Kühn, *RSC Adv.* **2015**, *5*, 85486–85493; b) J. F. Schlagintweit, C. Hintermeier, M. R. Anneser, E. M. H. Esslinger, S. Haslinger, F. E. Kühn, *Chem. Asian J.* **2020**, *15*, 1896–1902.
- [22] J. W. Kück, A. Raba, I. I. Markovits, M. Cokoja, F. E. Kühn, *ChemCatChem* **2014**, *6*, 1882–1886.
- [23] S. Haslinger, A. Raba, M. Cokoja, A. Pöthig, F. E. Kühn, *J. Catal.* **2015**, *331*, 147–153.
- [24] J. F. Schlagintweit, F. Dyckhoff, L. Nguyen, C. H. G. Jakob, R. M. Reich, F. E. Kühn, *J. Catal.* **2020**, *383*, 144–152.
- [25] M. A. Bernd, F. Dyckhoff, B. J. Hofmann, A. D. Böth, J. F. Schlagintweit, J. Oberkofler, R. M. Reich, F. E. Kühn, *J. Catal.* **2020**, *391*, 548–561.

Manuscript received: August 4, 2021

Accepted manuscript online: August 16, 2021

Version of record online: September 2, 2021
